Annu. Rev. Fluid Mech. 1999. 31:201–38

THE FLUID MECHANICS OF NATURAL VENTILATION

P. F. Linden
Department of Applied Mechanics and Engineering Sciences, University of California, San Diego, 9500 Gilman Drive, La Jolla, CA 92093-0411;
e-mail: pflinden@ames.ucsd.edu

KEY WORDS: wind, stack, mixing ventilation, displacement ventilation, stratification

ABSTRACT

Natural ventilation of buildings is the flow generated by temperature differences and by the wind. The governing feature of this flow is the exchange between an interior space and the external ambient. Although the wind may often appear to be the dominant driving mechanism, in many circumstances temperature variations play a controlling feature on the ventilation since the directional buoyancy force has a large influence on the flow patterns within the space and on the nature of the exchange with the outside. Two forms of ventilation are discussed: mixing ventilation, in which the interior is at an approximately uniform temperature, and displacement ventilation, where there is strong internal stratification. The dynamics of these buoyancy-driven flows are considered, and the effects of wind on them are examined. The aim behind this work is to give designers rules and intuition on how air moves within a building; the research reveals a fascinating branch of fluid mechanics.

1. INTRODUCTION

Humans have always sought shelter. In doing so the aim has been to extend the possibilities for living and working in inclement or inhospitable conditions. With the advent of the industrial revolution, continuing urbanization has led to an increased amount of time spent indoors. A building acts both as a barrier to the external environment and also as a window through which the outside is viewed. The quality of interior space is an increasingly important part of the environment, and modern designers make imaginative use of glass and

0066-4189/99/0115-0201$08.00

space to create well-lit and attractive interiors. These modern designs often create unusual conditions for ventilation: tall, open-plan spaces with large solar gains in which traditional "rules of thumb" for ventilation are not obviously applicable. Poorly designed naturally ventilated buildings are uncomfortable to live and work in and lead to reduced quality of life and loss of productivity.

In an attempt to optimize the internal quality particularly in terms of comfort and temperature, there has been an increasing move toward the use of air conditioning in modern buildings. This has undesirable energy implications and leads to high carbon dioxide emissions. In some cities, the air-conditioning requirements take almost the full capacity of the electricity grid. As a result there has been a reawakened interest in the use of natural ventilation to provide a high-quality indoor environment, both in commercial buildings and in industrial buildings which are subject to increasingly strict environmental and health regulations concerning air quality.

Natural ventilation uses the freely available resources of the wind and thermal energy that is a result of solar and incidental heating of the building. Although these resources are free, they are difficult to control. The challenge is to provide the necessary control mechanisms to develop the required indoor air quality. To achieve this, it is necessary to understand the physics of ventilation.

The main factors controlling indoor air quality are the air movement responsible for transporting both heat and pollutants and the building fabric, which influences the perceived temperature by radiative effects and by heat exchanges with the air. Of these two, air movement is less well understood and presents the greatest challenge to fluid dynamics. This review concentrates on the airflows generated by thermal and wind driving within buildings, and some remarks are made at the end concerning the linkages with the properties of the building fabric.

In general, even in relatively cold climates, buildings, especially modern constructions, are too hot. Activities within both the home and in commercial and industrial buildings use increasing amounts of energy; just count the number of electronic devices you have on standby! Modern buildings are tightly constructed with low leakage rates from materials that provide high thermal insulation. The design criteria for ventilation are based on the need to remove this excess heat (and pollutants) rather than provide adequate air for respiration. An individual requires about 7.5 liter/sec for respiration, while typical air changes needed for thermal comfort require at least ten times this amount.

The challenges facing the designer are complex and require an understanding of ventilation principles as well as skill in other facets of building design. The designer needs this understanding in an accessible form so that informed decisions can be made during the design phase of the building, whether a new construction or a retrofit. The questions posed in this process raise many

interesting, unanswered problems for the fluid dynamicist. In this review, I describe some of these problems and the way they have been addressed in terms of the fluid mechanics involved.

Ventilation is essentially the flow of air between the inside and outside of a building. This flow occurs through vents, traditionally windows, but increasingly through purposely designed, controlled openings not necessarily used for introducing light. These vents are usually sharp-edged orifices and pose little problem per se, but care must be taken in some circumstances, for example when air flows both in and out through a single vent (see Section 4).

The main problem concerns airflow patterns within the building. This may be a single space, but usually it is an interconnection of multiple spaces again connected by vents (often doorways). As a start it is simplest to consider the airflow within a single space, and most of the work to date has been on that aspect of ventilation. This approach is reasonable because an understanding of the single space is a crucial ingredient for multiply connected spaces, but as we will see, the latter raise interesting new problems that deserve further study.

The early work on natural ventilation centered on wind-driven flows and was, and still is, extensively studied in wind tunnels. Models of buildings are placed in an airstream and the pressure distributions around the building are measured for various orientations of the incident wind. Pressure coefficients are determined and these are used to calculate the flow through vents at different locations on the façade. The results are either applied directly from the wind tunnel tests to the full-scale building, or empirical values are given depending on the location on the building (Dascalaki & Santamouris 1996). From this information, flow rates through the building are related to the wind speed. There is little consideration of flow patterns within the building or the mechanics of the flow.

As a result of the problems associated with overheating, recent interest has begun to focus on flows driven by temperature differences. It is envisaged that 'worst case' conditions arise on hot, windless days when all the ventilation is driven by buoyancy forces. However, such 'worst case' considerations place very large demands on designs that may not be necessary for an efficient, naturally ventilated building. For example, if 'worst case' conditions only occur a few times per year and then for only part of the day, it may be economically beneficial to accept a small loss in usable time or a period of less acceptable indoor air quality rather than pay for energy costs of a mechanical or air conditioned system for the rest of the year. Even mechanical ventilation systems use design criteria based on maintaining comfort conditions for a proportion of the year only. Other options include hybrid systems, part mechanical and part natural, but these will not be discussed here.

Thus it is necessary to consider the combinations of wind and buoyancy. Even in the case of a single space, the flows induced can be very complex; models are

only now being developed to calculate them. For multiply connected spaces, there is no comprehensive model or characterization of the likely flows to be encountered (see Section 8.2).

The format of this review is as follows. The next two sections will discuss wind-driven and buoyancy-driven ventilation. Single-sided ventilation will be examined in Section 4, and some effects of wind on the stack-driven flow will be discussed. More general consideration of the combined effects of stack and wind will be given in Section 5. The use of computational fluid dynamics is described in Section 6, and some non-Boussinesq effects associated with the ventilation of fires are discussed in Section 7. Finally, Section 8 will describe some of the outstanding issues concerning complex effects such as effects of the building fabric, multiply connected spaces, unsteady flows, and other issues concerning heat sources.

2. WIND-DRIVEN VENTILATION

The effect of wind on a building is dominated by the shape of the building and the proximity of other buildings. Broadly speaking, pressures are higher on the windward side of the building and lower on the leeward side and on the roof and so will tend to drive a flow within the building from the windward vents to the leeward vents. Consequently, attention has been focused on how these pressure differences vary with building shape, wind direction, and the presence of nearby buildings. Because separation is a major factor in determining the wind flow around the building, particularly downstream of the windward face, and most buildings have sharp corners, wind speed plays only a minor part in determining the air flow pattern around the building, which is governed by inviscid dynamics. This independence of Reynolds number is, of course, why wind-tunnel modeling has been so successful in determining airflow characteristics.

Much of the early work on the interaction of wind with buildings has been concerned with aerodynamic loading (Owen 1971). Full-scale measurements of urban wind conditions (Evans & Lee 1981, Cook et al 1974) show that modifications to the free-stream velocity due to nearby buildings are extremely complicated; as yet, no general theory has been developed to address this question. Wind-tunnel measurements (Hussain & Lee 1980) show that the flow in a regular array of cubes has a range of properties depending on the spacing of the obstructions within the array. Consequently, recourse is usually made to wind-tunnel measurements to determine wind pressure coefficients at particular locations on the building of interest. Surrounding buildings are included in the wind-tunnel model, and it is generally accepted that, provided the wind tunnel satisfies certain requirements, the pattern of the flow, the distribution of wind speeds around a properly scaled model and, consequently, the distribution of

wind pressures on the external surface of the model are equivalent to that on a full-scale building. The requirements for accurate wind-tunnel modeling are that the velocity profile in the on-coming airstream represents the atmospheric boundary layer structure flowing over terrain similar to that of the site under consideration and that the distribution of turbulence scales in the wind tunnel should be similar to that at full scale with the appropriate reduction in the size of turbulent eddies for the small-scale model. Typically, models are 1:200 in scale, and various devices are used to trip the boundary layer and to provide the required vertical profile and turbulence structures. These include the use of bi-planar grids to generate turbulence and various empirical uses of roughness and fences upstream of the model. Pressure tappings are located over the surface of the building and the pressures P measured on the surface of the building are related to the reference pressure P_{ref}, which is measured in the wind tunnel at a location well upstream of the model. Pressure coefficients $C_p = P/P_{ref}$ are defined by

$$P = \frac{1}{2}\rho C_p U^2, \tag{1}$$

where ρ is the air density. Usually the model is located on a rotating platform that enables different wind directions to be tested and pressure coefficients to be determined over the full range of wind directions.

For buildings with sharp edges, where the wind separates, this information can be used to calculate the pressure distribution at full scale for the full range of wind speeds and directions. This information is then used to calculate the pressure change across any opening and the flow driven through the opening according to

$$Q = AC_D \left[2\frac{\Delta P}{\rho}\right]^{\frac{1}{2}}, \tag{2}$$

where A is the area of the opening, ΔP is the pressure drop across the opening, and C_D is a discharge coefficient associated with the opening (see Section 4).

The presence of buildings can intensify turbulent fluctuations present in the air flow by vortex stretching processes (Britter et al 1979). This process is even more complicated in groups of buildings with the possibility of unsteady effects in the wakes interacting with the buildings further downstream. However, there seems to be no systematic study of these turbulence effects on the wind-driven flow, or even estimates of the likely timescales for their impact on ventilation. One exception to this is the work of Wilson & Keil (1990), discussed in Section 4.

3. STACK-DRIVEN VENTILATION

Temperature differences between the inside and outside of a building and between different spaces within a building produce buoyancy forces that drive flow. In contrast to the purely wind-driven case, the presence of these buoyancy forces leads to temperature variations within the space. This stratification may lead to quite different flow configurations. The natural tendency for hot air to rise and accumulate toward the upper part of the space leads to a stable stratification, and this has a large influence on the flow patterns within the space.

The determining factor in the form of the vertical stratification is the location of the openings. If the air in the space is warm compared to the environment, then a single opening at the top of the space (Figure 1*a*) will allow exchange of warm air outwards and cool air inwards. The incoming cool air will descend as a turbulent plume that will tend to mix the air within the space. This type of ventilation is known as mixing ventilation and is characterized by a relatively uniform interior temperature distribution.

If the single opening is located at the lower part of the space, there will be a transient exchange until the cool incoming air occupies a depth up to the top of the opening, after which further ventilation ceases. This is not, in general, an efficient way of ventilating.

If two vents are open, one near the top of the space and the second near the bottom of the space (Figure 1*b*), warm air flows out through the upper opening and cool air enters through the lower opening. A stable density interface

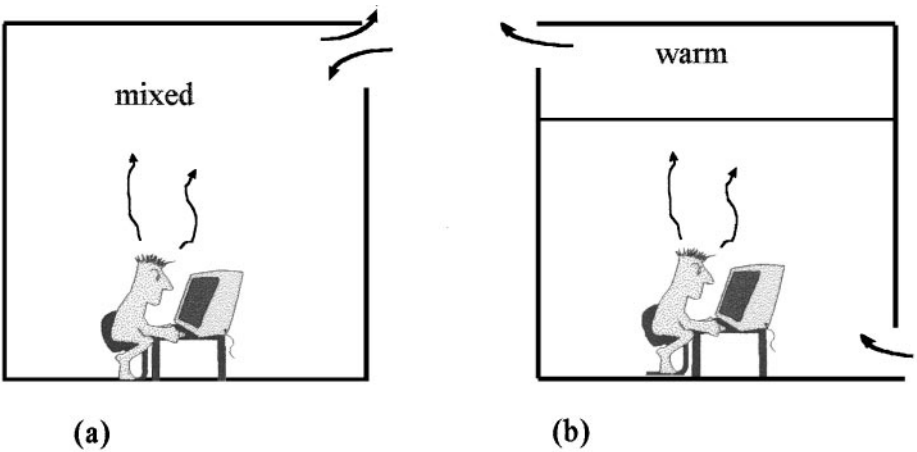

Figure 1 Schematics of mixing ventilation (*a*) and displacement ventilation (*b*).

forms between the warm, upper layer and the cooler, incoming air. This form of ventilation is known as displacement ventilation. It is characterized, in contrast to mixing ventilation, by large temperature variations within the space. For the same temperature difference and vent area, displacement ventilation leads to more rapid ventilation than mixing ventilation. This latter result is an example of the importance of flow patterns to the efficiency of the ventilation system.

3.1 *The Neutral Level*

Consider the situation shown in Figure 2, where the exterior density ρ_{amb} is constant and the interior density of the space is $\rho_s(z)$. In the absence of motion, the pressure is hydrostatic, $\frac{dp}{dz} = -g\rho$. When the interior is warmer than the exterior $\rho_s < \rho_{amb}$, the pressure gradient inside the space is less than that in the ambient and is represented schematically as shown, where the pressure in the ambient is p_0 at $z = 0$ and p_H at $z = H$. Let $0 < z_1 < H$ be the level at which the pressure inside the space equals the ambient pressure at that height. The higher internal pressure at the upper opening drives outflow and the lower internal pressure at the lower opening drives inflow. Thus the neutral level defines the height that separates lower and upper openings: air flows out through openings above the neutral level (upper openings) and in through openings below the neutral level (lower openings). This has important implications when designing for the ventilation of smoke from a fire, as the upper vents must be above the neutral level (see Section 7).

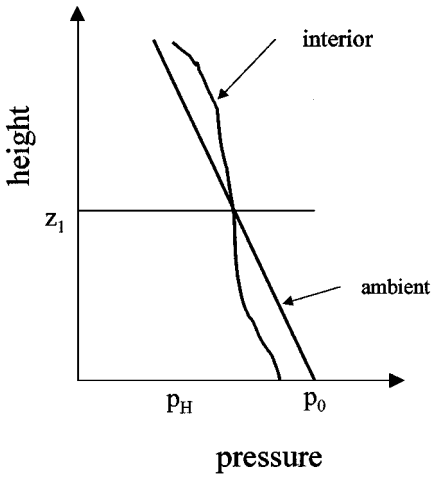

Figure 2 Pressure distributions and the neutral level.

3.2 *Laboratory Simulations*

In contrast to wind-driven ventilation it is difficult to carry out studies of stack-driven ventilation at small scale because of the increased importance of viscous effects at the lower Reynolds numbers obtained. Consequently, most direct studies have been carried out at close to full scale (Lane-Serff 1989) and have, so far, been restricted to flow in a single space—sometimes partially divided.

In order to overcome this problem, the group at Cambridge have developed the methodology of small-scale modeling using water as the working fluid (Linden et al 1990, Baker & Linden 1991). Buoyancy forces are produced by salinity differences within the fluid. The buoyancy force is most conveniently described in terms of a reduced gravity g' defined as

$$g' = g\frac{\Delta\rho}{\rho} = g\frac{\Delta T}{T}, \tag{3}$$

where g is the acceleration of gravity and $\frac{\Delta\rho}{\rho}$ is the fractional change in density produced by a temperature difference $\frac{\Delta T}{T}$, where T is measured in Kelvin. The dimensionless parameters of concern are the Reynolds numbers $Re = \frac{UH}{\nu}$ and the Peclet number $Pe = \frac{UH}{\kappa}$, where ν is the kinematic viscosity, κ is the coefficient of molecular diffusivity, and H is a typical vertical scale.

For flows driven by a reduced gravity g', the velocity U scales on $(g'H)^{1/2}$ and so $Re = \frac{(g'H)^{1/2}H}{\nu}$ and $Pe = \frac{(g'H)^{1/2}H}{\kappa}$. Small-scale laboratory experiments reduce H by at least a factor of 10, and using air as a working medium, the Reynolds and Peclet numbers are reduced by at least a factor of 30 from the values at full scale. Working with salinity differences in water allows larger values of g' and has smaller values of ν and κ, and so full-scale values of *Re* and *Pe* can be achieved.

In both the small-scale and full-scale flows, both *Re* and *Pe* have values in excess of 10^3, and the flow is independent of viscous and diffusive effects, except at very small scales. Quantitative comparisons between laboratory models and full-scale measurements (Lane-Serff 1989 and Savardekar 1990) confirm that large-scale flows are accurately represented at small scales.

Flows driven by sources of heat with heat flux W are characterized by the buoyancy flux B

$$B = \frac{g\gamma W}{\rho c_p}, \tag{4}$$

where $\gamma = \frac{1}{T}$ is the coefficient of expansion and c_p the specific heat capacity at constant pressure. (It is useful to note that the buoyancy flux due to a heat flux of W (kilowatts) in air at room temperature is $B = 0.0281W$, where B is measured in $\mathrm{m}^4\,\mathrm{s}^{-3}$.)

Table 1 The scaling relations between model and full scale for stack-driven flows

Scale	Model	Full scale
Times	$(L_m/g'_m)^{\frac{1}{2}}$	$(L_f/g'_f)^{\frac{1}{2}}$
Velocities	$(L_m g'_m)^{\frac{1}{2}}$	$(L_f g'_f)^{\frac{1}{2}}$
Buoyancy fluxes	$L_m^{5/2} g_m'^{3/2}$	$L_f^{5/2} g_f'^{3/2}$

The relation between the experimental results and the real situation is found by considering appropriate scalings. The subscripts $_m$ and $_f$ are used to denote the scales in the model and real (full-scale) cases, respectively. Length scales are denoted by L, velocities by U, times by t, and buoyancy flux by B. (The buoyancy flux is the flux of g'.) These scales can be constructed from the length scale and g', as shown in Table 1. Thus, for example, the ratio of velocities in an experiment to those at full-scale is

$$(L_m\ g'_m)^{\frac{1}{2}} : (L_f\ g'_f)^{\frac{1}{2}}. \tag{5}$$

For typical experiments, $L_m/L_f = 1/25$ and density differences are such that $\Delta\rho/\rho = 0.01$ corresponds to, say, a temperature difference of 5°C. Then timescales in the model range from about 2 times faster that at full scale for internal gains of 50 W m^{-2} to about 3 times faster for gains of 10 W m^{-2}.

In addition to achieving dynamic similarity, the use of water as a working fluid has other advantages. The first is that it is very easy to do simple flow visualization using dyes and shadowgraphs in order to see flow patterns and density variations. Second, quantitative measurements of flow velocities and temperature measurements can be made using digital image-processing techniques (Hacker et al 1996; GR Hunt & PF Linden, submitted). Furthermore, imagery of the flow is a very useful way of imparting information to designers concerning the consequences of various design changes.

Recently it has been possible to extend this technique to the case of temperature differences in water. Although it is not possible to obtain such large values of g' in this case, recent measurements have shown that the quantitative agreement between the temperature stratified experiments and the salt stratified experiments is very good. This agreement implies that sufficiently high Reynolds numbers and Peclet numbers are achieved using heated water. This allows the possibility of using different boundary conditions such as heated or cooled walls in order to simulate other effects of natural ventilation (see Section 8.3 and Sandberg & Lindstrom 1990).

3.3 *Mixing Flows*

Mixing ventilation occurs when cold air enters at high level or warm air enters at low level. As shown in Figure 1*a*, this situation can be most simply modeled by a single opening of area A through which there is an exchange flow (see Section 4) with a volume flux

$$Q = C_D A (g' H)^{\frac{1}{2}}. \tag{6}$$

Assuming that the incoming plume maintains mixed interior conditions, this exchange flow causes an interior space with volume V and initial buoyancy g'_0, to change temperature according to

$$\frac{\mathrm{d}g'}{\mathrm{d}t} = -\frac{g'Q}{V}. \tag{7}$$

Hence

$$\frac{g'}{g'_0} = \left(1 + \frac{t}{\tau}\right)^{-2}, \tag{8}$$

where the mixing timescale τ is

$$\tau = \frac{2V}{C_D A}(g'_0 H)^{-\frac{1}{2}}. \tag{9}$$

Sources of buoyancy with buoyancy flux B will lead to a steady interior temperature g'_s, given by

$$B = g'_s Q, \tag{10}$$

and so

$$g'_s = \left(\frac{B}{C_D A H^{\frac{1}{2}}}\right)^{\frac{2}{3}}. \tag{11}$$

3.4 *Displacement Ventilation*

3.4.1 DRAINAGE FLOW UNDER DISPLACEMENT VENTILATION For the situation shown in Figure 1*b*, there will be outflow at the upper vent and inflow at the lower vent. These velocities can be calculated by Bernoulli's theorem by defining pressures relative to the neutral level (see Section 3.1). This analysis implies the volume flux through the space is given by

$$Q = A^*[g'(H - h)]^{\frac{1}{2}}, \tag{12}$$

where h is the interface height above the floor, H is the height of the space, g' is the buoyancy jumps across the interface, and A^* is the effective area given

by (16). For a uniform space with floor area S internally filled with fluid of buoyancy g_0', the interface height h satisfies

$$\frac{h}{H} = 1 - \left(1 - \frac{t}{t_e}\right)^2, \tag{13}$$

where the time t_e for the space to empty is given by

$$t_e = \frac{2S}{A^*}\left(\frac{H}{g_0'}\right)^{\frac{1}{2}}. \tag{14}$$

Comparison with the mixing ventilation time τ given by (9) shows that, for a space of uniform cross-sectional area, $\frac{t_e}{\tau} \approx C_D \approx 0.6$, and so emptying times are significantly shorter for displacement ventilation.

3.4.2 SINGLE SOURCE OF BUOYANCY Displacement ventilation with a source of buoyancy was first discussed by the Swedish group under Sandberg (Sandberg & Lindstrom 1987, 1990). They considered the case of mechanical ventilation, where the flow rate through the space is specified, for example by the output from a fan, and were the first to appreciate that this configuration leads to a two-layer stratification, with the height of the interface between the layers set by matching the volume flowrate in a heated plume with that imposed by the fan. They also pointed out several advantages of displacement ventilation over mixing ventilation, especially the efficient flushing of pollutants from the space.

The connection to the environment through natural ventilation was made by Linden et al (1990), who investigated the flow in an enclosure with high-level and low-level openings generated by a single point source of buoyancy on the floor of the enclosure (see Figure 3). They showed that in this case a very simple stratification develops consisting of two layers separated by a horizontal interface. The lower layer is at uniform ambient temperature and the upper layer is also at a uniform but higher temperature that depends on the buoyancy flux from the source. The dimensionless depth of the cool ambient layer $\xi = h/H$ is given by

$$\frac{A^*}{H^2} = C^{\frac{3}{2}}\left(\frac{\xi^5}{1-\xi}\right)^{\frac{1}{2}}, \tag{15}$$

where A^* is the "effective" area of the top and bottom openings of the enclosure, and H is the height difference between the top and bottom openings. The constant $C = \frac{6}{5}\alpha(\frac{9}{10}\alpha)^{\frac{1}{3}}\pi^{\frac{2}{3}}$, where α is the (top-hat) entrainment constant for the plume, is given by the plume theory of Morton et al (1956).

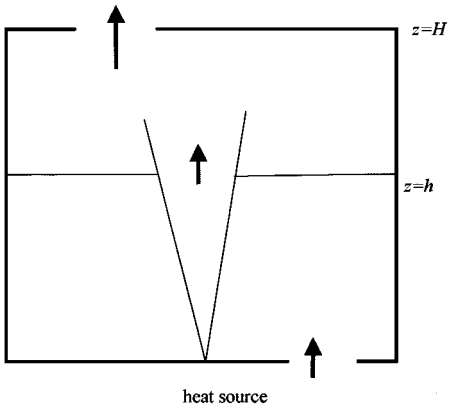

Figure 3 Displacement ventilation with a single source of buoyancy.

The effective area A^* of the openings is defined as

$$A^* = \frac{c_d a_t a_b}{\left(\frac{1}{2}\left(\frac{c_d^2}{c} a_t^2 + a_b^2\right)\right)^{\frac{1}{2}}}, \tag{16}$$

where a_t and a_b are the areas of the top and bottom openings, respectively, and c is the pressure loss coefficient associated with the inflow through the lower sharp-edged opening. A discharge coefficient c_d is used here to account for the vena contracta at the downstream side of the sharp-edged upper vents. If there are n sources of equal strength present on the floor of the enclosure, again a stratification with two uniform layers forms, and since each source shares an equal fraction of the effective area A^*, the nondimensional height ξ of the interface is given by

$$\frac{1}{n}\frac{A^*}{H^2} = C^{\frac{3}{2}}\left(\frac{\xi^5}{1-\xi}\right)^{\frac{1}{2}}. \tag{17}$$

In the single plume case, or when the sources have equal strength, the height of the interface is independent of the buoyancy fluxes and depends only on the dimensionless vent area A^*/H^2. On the other hand, the temperature of the upper layer, which is independent of height, increases as the heat flux of the plumes increases. The result (15) had previously been derived by Thomas et al (1963) for the case of a (Boussinesq) fire plume, a fact not known to me at the time we published the work on displacement ventilation.

These results provide some simple guidelines for the designer. Equations (15) and (17) show that in order to achieve a deep layer at ambient temperature

($\xi \to 1$), it is necessary to have a very large area of openable vents. In practice, this is extremely difficult to achieve, and consequently it is a good idea to have some dead space at the top of an enclosure in which the hot air can accumulate in order to drive the flow. The flow through the system is controlled by the effective area (16), and the magnitude of A^* is determined by the smaller vent area. For example, when $a_t \ll a_b$, $A^* \to a_t c_d \sqrt{2}$, and so control of the flow can be achieved by adjusting the smaller openings to the enclosure. Possibly the most important property of these flows is that the interface height is independent of the strength of the buoyancy flux from the source, which results from the fact that the position of the interface is governed by the entrainment into the plume. Thus design considerations that aim at ensuring the hot layer is above the occupied zone of a space are independent of the heat flux.

3.4.3 MULTIPLE SOURCES OF BUOYANCY Thermal stratification (or stratification of contaminant concentration) in practical situations does not generally exhibit a sharp change in density between two internally well-mixed layers as described in the simple model above. A more gradual change from ambient conditions at the bottom of the enclosure to a maximum temperature at the top is observed (e.g. see Gorton & Sassi 1982, Jacobsen 1988, Cooper & Mak 1991). This type of stratification arises from many factors not included in the simplified model of a single plume within the space. In practice, heating is from distributed sources of buoyancy of different strengths, located at various positions within the space.

In an attempt to address this issue, the approach of Linden et al (1990) has been extended to cover multiple source of buoyancy of different strengths. The fluid mechanics is similar to the single-source case, but the analysis is complicated by the fact that the stronger plumes rise through a stratified region and discharge their buoyancy at higher levels within the space.

3.4.3.1 *Two sources of buoyancy* A schematic of two positive sources of buoyancy is shown in Figure 4. A three-layer stratification occurs in this case, and the dimensionless interface heights are given by

$$\frac{A^*}{H^2 C^{\frac{3}{2}}} = \frac{(1+\psi^{\frac{1}{3}})^{\frac{3}{2}}}{(1+\psi)^{\frac{1}{2}}} \left(\frac{(h_1/H)^5}{1 - h_1/H - \frac{(1-\psi^{\frac{2}{3}})}{(1+\psi)} \left(\frac{h_2 - h_1}{H}\right)} \right)^{\frac{1}{2}} \tag{18}$$

and are shown in Figure 5 (see Cooper & Linden 1996). Here $\psi = B_1/B_2 \leq 1$ is the ratio of the buoyancy fluxes of the two plumes. This relationship is of a very similar form to that for a single plume (16). As before, the interface heights are independent of the total buoyancy fluxes and depend only on the

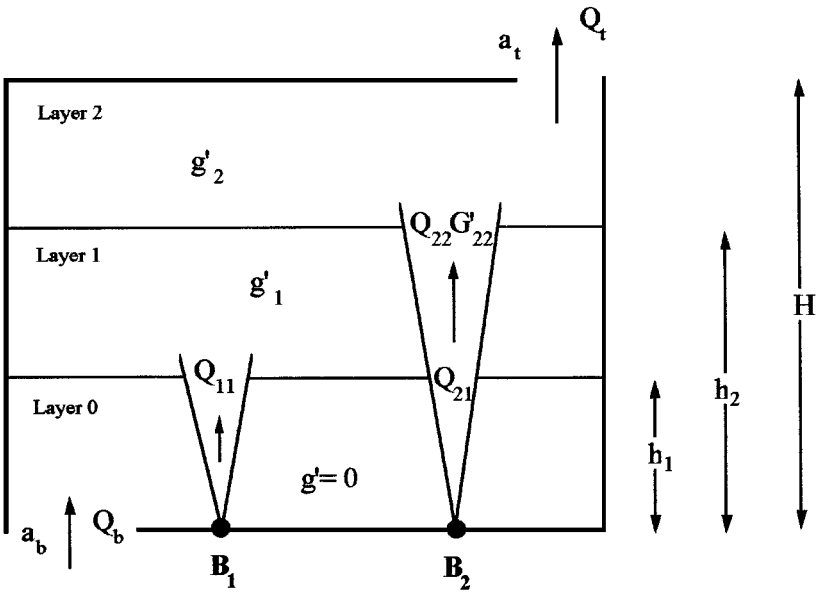

Figure 4 Displacement ventilation with two positive sources of buoyancy.

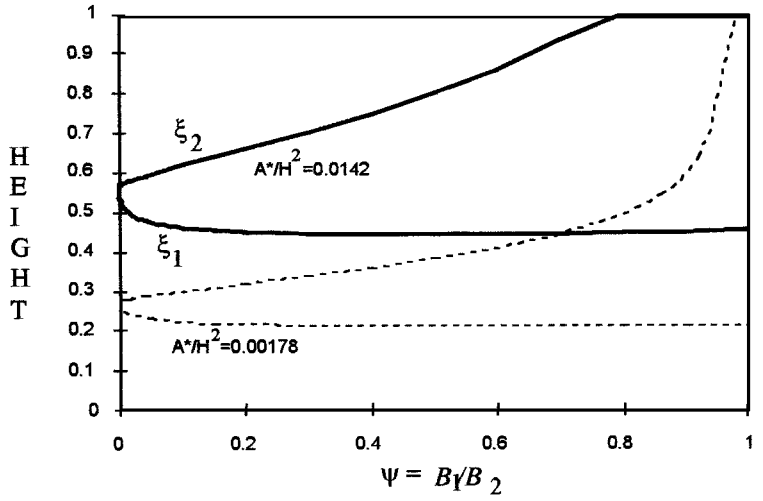

Figure 5 Theoretical prediction of the nondimensional interface heights h_1/H and h_2/H as functions of the ratio B_1/B_2 of the buoyancy fluxes, for two different values of the dimensionless vent area A^*/H^2.

openable areas of the vents, the height of the enclosure, and the ratio ψ of the buoyancy fluxes. The latter dependence reflects the facts that the interface positions depend on entrainment into the plumes and that the distribution of the buoyancy between the two plumes is a crucial factor in determining the form (but not the strength) of the stratification.

As shown by (18), the interface heights depend only on the dimensionless area A^*/H^2 and the ratio ψ of the buoyancy fluxes. When $\psi = 0$, a single interface forms, and for $\psi > 0$ this interface splits into two with the lower interface ξ_2 descending as ψ increases. The buoyancy of the intermediate layer increases relative to that of the upper layer as ψ increases, and the two are equal when $\psi = 1$. At this point, or before as a result of entrainment by the weaker plume, the interface ξ_2 disappears and the result for two equal plumes given by (17) with $n = 2$ is obtained.

A three-layer stratification also occurs when there is one positive and one negative source of buoyancy (Cooper & Linden 1995). This flow models the ventilation flow with a chilled ceiling. In this case, when the net buoyancy flux into the space is close to zero because of equal strength plumes, the ventilation flow is weak and will be strongly influenced by wind (Section 5). In some circumstances the falling and rising plumes may collide, but it appears that mixing between the plumes is relatively weak (Kaye 1998).

3.4.3.2 *Multiple plumes* An approximate model, which ignores the effects of stratification on the plumes, has been developed by Linden & Cooper (1996). It is assumed that a layered stratification develops and the strength of the stratification above the ambient zone is determined by the relative strengths of the individual plumes. For example, consider the case of n plumes where

$$B_i = \frac{i\beta}{n} B \quad (i = 1, \ldots, n-1, \beta = \text{constant} \leq 1)$$
$$B_n = B. \tag{19}$$

The case for 10 plumes with $\beta = 0.1$ is shown in Figure 6. Note that a gradual transition in temperature occurs in the region above the ambient zone, which is more in keeping with the observed temperature profiles in buildings.

From a design viewpoint, the height of the lowest interface is the critical parameter, as this determines the depth of the zone at ambient temperature, and the depth of the ambient zone is very sensitive to the number of sources. Thus, distributing the buoyancy flux from a single source into 10 equal sources reduces the height of the ambient zone by a factor of about 2. The calculations with multiple plumes show that the height of this interface is well approximated by the n equal plumes result (17) for a wide range of buoyancy fluxes (see Figure 5). Current fire design guidelines are generally based on a single source

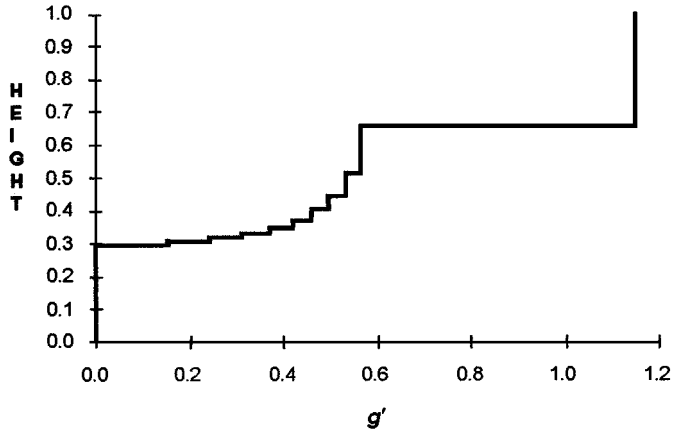

Figure 6 The stratification produced by $n = 10$ plumes, with strengths given by the arithmetic progression (19), plotted against the dimensionless height within the enclosure. The strength of the stronger plume is 20 kW, the dimensionless vent area $A^*/H_2 = 0.0167$, $H = 5$ m, and $\alpha = 0.1$. Note that $g' = 1$ m s^{-2} corresponds to a temperature difference of about 30°C.

of heat or smoke in a space. These results show that the height of the smoke-free zone in a naturally ventilated space will decrease significantly in the event of two or more fires.

3.4.4 DISTRIBUTED SOURCES There are many situations, especially involving solar gains, where the sources of buoyancy are distributed over a surface. For a horizontal surface it is possible to consider the plume as arising from a virtual origin at a different height from the floor. This situation enables the results of Section 3.4.2 to be used with some minor modifications (Caulfield 1991). For the case of a distributed source on a vertical wall the situation is more complicated. With displacement ventilation a steady state will form, but if an interface forms at any height then the flux through the space will be the same as the flux in the plume crossing the interface. Since the plume from a distributed vertical source will increase due to the addition of more buoyancy, then the possibility exists that a series of layers will form. At any level where the volume flux in the plume is not equal to the volume flux out of the space, there must be a net vertical motion exterior to the plume, and for a steady state, fluid elements exterior to the plume must move along surfaces of constant density. The theory described in Section 3.4.2 can easily be extended to consider this case, and for small A^*/H^2 the number of layers is given by

$$N(N+1)^5 = \alpha^3 \pi^2 \frac{H^4}{A^{*2}}. \tag{20}$$

Experiments by Linden et al (1990) and more recently by P Cooper (personal communication) suggest that intermediate layers do form in this case, but considerably more work needs to be done to verify (20).

A cross between mixing and displacement ventilation occurs when there are low and high level openings (so that displacement ventilation is expected) and the heat flux in the space is uniformly distributed over the whole area of the floor. This is the limit of an infinite number of plumes, and the interface reaches the floor so that the whole interior is at a uniform temperature. The pressure differences from top to bottom of the space is then $(g'H)^{\frac{1}{2}}$, and so the flow through the space has volume flux

$$Q = A^*(g'H)^{\frac{1}{2}}. \tag{21}$$

In the steady state, the total buoyancy flux into the space is $B = g'Q$, and hence the uniform buoyancy is

$$g' = \left(\frac{B}{A^*H^{\frac{1}{2}}}\right)^{\frac{2}{3}}. \tag{22}$$

This result is equivalent to the mixing-flow solution (11).

3.5 *Heat Recovery*

A major concern in ventilation systems is the loss of heat from the building in winter. Heat recovery can be achieved by recirculating air from the outlet to the inlet of a displacement system, as shown in Figure 7.

In the above case of a single heat source with heat flux W, provided $Q_A \neq 0$, a steady state is produced in which the height of the interface is given by

$$\frac{A^*}{H^2} = C^{\frac{3}{2}}\xi^{\frac{5}{2}}(1-r)\left(1-\xi-\frac{r}{1-r}\right)^{-\frac{1}{2}}, \tag{23}$$

where $r = \frac{Q_R}{Q_R+Q_A}$ is the fraction of the total volume flux through the space that is recirculated. The temperature of the lower layer is given by

$$T = T_A + \frac{1}{C}(g\alpha)^{-\frac{1}{3}}(W/\rho c_p)^{\frac{2}{3}}h^{-\frac{5}{3}}\frac{r}{1-r}, \tag{24}$$

and the temperature difference ΔT across the interface is given by

$$\Delta T = \frac{W}{\rho c_p(Q_A+Q_R)}. \tag{25}$$

These results reduce to those given in Section 3.4.2 for the case of no recirculation ($r = 0$) and show that as the proportion of the ventilation recirculated is increased, the height of the interface increases as does the temperature of the lower layer. This, therefore, provides a mechanism for using recovered heat to warm the ambient air in winter to provide a more comfortable occupied zone while still retaining the advantages of displacement ventilation.

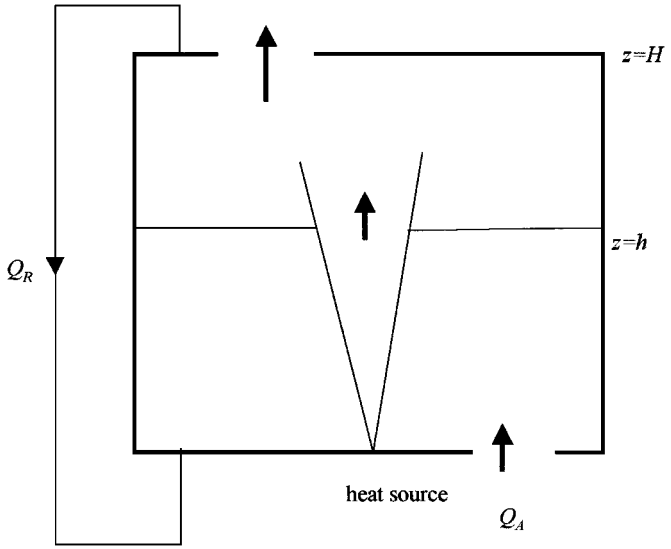

Figure 7 Displacement ventilation with heat recovery.

4. SINGLE-SIDED VENTILATION

Single-sided ventilation is one of the more common forms of natural ventilation and occurs when there is a single opening into a space. It may take the form of either mixing or displacement ventilation depending on the position of the opening. Early work on this flow was a theoretical and experimental study of the exchange flow through a rectangular opening in a vertical wall of height H and area A by Brown & Solvason (1962a,b), who showed that the flowrate Q through the openings is given by

$$Q = \frac{1}{3} C_D A (g' H)^{\frac{1}{2}}, \tag{26}$$

where C_D is a discharge coefficient accounting for streamline contraction and taking values of 0.6 (sharp orifice), 0.8 (short tubes), and 0.98 (streamline shapes). They carried out experiments on single and double openings in a vertical partition between two spaces and found good agreement with (26). The same result was found by Shaw & Whyte (1974)—see also Linden & Simpson (1985) and Lane-Serff et al (1987). The flow through the opening is a two-layer exchange flow. For a symmetrical opening the interface is at the mid height of the opening, and since the flow is density driven, there is negligible mixing between the two layers. An explanation of (26) in terms of hydraulic control was given by Dalziel & Lane-Serff (1991), who showed that

the flow is critical at the opening. This insight allows the result to be applied to nonsymmetrical openings, such as a doorway flush with the floor but with a sofit to the ceiling, in which case the interface between the two-layer flow is not located midway up the opening, and the flowrate is modified accordingly.

Wilson & Keil (1990) carried out experiments on the exchange flow through a window in a heated, sealed room of a test house. They found that their data gave smaller values of the discharge coefficient $C_D \approx 0.044 + 0.004\Delta T$, where ΔT is the temperature difference across the opening, and suggested that the reduction was caused by mixing of the incoming and outgoing air at the window. This view is supported by their vertical temperature profiles, which show smoother transitions at low ΔT and a more two-layer structure at high ΔT. However, as they point out, the flow rate is also affected by the wind speed, with less exchange at higher speeds. This reduction in the exchange flow may result from higher turbulence levels as the wind speed increases. The turbulence disrupts the organized two-layer exchange, leading to mixing between the layers and a less efficient flow through the opening.

The exchange flow rate through a full-height doorway at the end of a corridor (closed at the other end) in the presence of a headwind has been studied by Davies & Linden (1992). In the case of zero wind and a warm corridor, there is an exchange flow through the doorway with the incoming cold air travelling along the floor as a gravity current that occupies half the depth of the corridor (Linden & Simpson 1985). When the current hits the end of the corridor, a reflected bore travels back toward the doorway as the warm air continues to drain. The effect of the wind U is characterized by the Froude number $Fr = U/(g'H)^{1/2}$, where H is the height of the corridor and g' the initial buoyancy difference. As Fr increases, the interface in the doorway increases in height above the mid-point as a result of the larger stagnation pressure. For large $Fr \approx 10$, the flow in the doorway is observed to be turbulent with significant mixing between the incoming and outgoing airstreams. Measurements show the rate of exchange of air through the doorway decreases with increasing wind speed (increasing Fr). This is explained by the fact that as the interface moves toward the top of the doorway, the speed of the outflowing warm air increases; hence, the shear across the interface increases until the local Richardson number Ri becomes small enough to allow shear instability. Estimates show that $Ri < 0.25$ when $Fr \geq 6$, a result consistent with the flow observations. Similar results were also obtained for headwinds incident at angles up to 40° to the axis of the corridor.

Davies (1993) also studied the case in which there is a continuous source of buoyancy with flux B_L per unit width in the corridor. In this case, the Froude number $Fr = U/B_L^{1/3}$. In the absence of wind ($Fr = 0$), a two-layer stratification is established in the corridor with an exchange flow at the doorway at

which the volume flux (from entrainment into the plume) and buoyancy flux are in balance. This flow is similar to buoyancy-driven flows in semi-enclosed seas such as the Red Sea (Maxworthy 1997), where there is buoyancy input over the sea surface and the flow is controlled at an opening such as a strait. As *Fr* increases, the interface rises near the doorway, but remains unaltered within the corridor. Some mixing near the doorway is observed, and for larger values of *Fr* the flow is turbulent and there is substantial mixing between the incoming and outflowing air. This mixing region occupies a region of length $0(H)$ near the doorway, beyond which the two-layer stratification is established.

This situation is quite different from the transient drainage flow since it is controlled by the buoyancy and volume fluxes in the plume, and the exchanges at the doorway adjust to supply these. Consequently, although the flow takes a different form in the doorway with increasing mixing at higher *Fr*, there is not a large difference in the exchange flow with wind speed.

Similar effects are also found on exchange flows in the use of intentional forcing such as air curtains (Davies 1993) or water spray barriers to mitigate the effects of fires (Linden et al 1992). Air curtains, usually consisting of warm air blown downward near a doorway, are used to reduce the loss of heat from the interior; these devices are commonly used in shops. The flow is dominated by the downward momentum in the jet, and this mixes the exchange flow in the doorway, reducing it in similar manner to that observed with a headwind (see also Linden & Simpson 1987). However, as in the headwind case, there is ultimately no reduction when the steady flow associated with continuous buoyancy sources in the interior is considered, because the sources control the exchange flow. So air curtains do not save energy, although they may encourage shoppers to enter shops! Similarly, the water spray barrier does not ultimately reduce the outflow from a fire (although the water provides some additional cooling), but it does delay the propagation of the smoke-filled gravity current. Similar effects on exchange flows are produced by turbulence in the exterior flow—see Keil (1991) and the discussion of Wilson & Keil (1990) earlier in this section.

4.1 *Openings in Non-Vertical Walls*

The exchange flow described above applies to an opening in a vertical wall. On sloping surfaces, or horizontal roofs, dimensional analysis suggests that (26) still applies, but now the discharge coefficient $C_D = C_D(\theta)$, where θ is the angle the slope makes with the horizontal. For an opening in a horizontal surface ($\theta = 0$), Brown et al (1963) and Epstein (1988) found that $C_D(0) = 0.15$, which is about 25% of the exchange for the same size opening in a vertical surface. In this case, the interface is unstable to Rayleigh-Taylor instability and there is significant mixing between the up- and down-flowing air as it passes through the openings. Keil (1991) and Davies (1993) investigated the behavior for

intermediate angles and observed that for $\theta < 4^\circ$ the strongly mixed exchange flow was observed, C_D remains constant until $\theta \approx 4$–5° and then increases with θ, reaching a constant value $C_D = 0.6$ for $\theta \geq 20^\circ$, at which point a two-layer exchange flow is established with no significant mixing.

5. COMBINED EFFECTS OF WIND AND BUOYANCY

The above discussion of single-sided ventilation has shown that the effect of wind may not necessarily lead to increased ventilation in the presence of buoyancy. This is clearly an undesirable feature in many situations, as the object of the design is to provide adequate ventilation over a wide range of wind- and stack-driven conditions. We now consider the case of displacement ventilation in the presence of wind, extending the discussion of Section 3 to that case. When there is warm air inside the space and the stack-driven flow drives this warm air outward through the upper openings and introduces ambient cooler air through the lower openings, the effect of an incident wind field will be reinforcing if the lower vents are on the windward side of the building and the upper vents are on the leeward side. If the opposite is true, then the wind-driven flow will be opposed to the stack-driven flow and in general the ventilation is less efficient. The effect of the wind may be represented by a 'wind-pressure drop' Δ defined by $\Delta = \frac{1}{2}\rho U^2$, which is the pressure difference between the windward and leeward openings associated with a wind speed U. In this section we discuss how these flows may be analyzed and also look at the relative importance of wind- and stack-driven ventilation in both cases.

5.1 *Reinforcing Wind and Buoyancy Forces*

5.1.1 DRAINAGE FLOW When warm air is escaping from an upper, leeward vent and cool air is entering from a lower, windward vent, the wind-driven flow reinforces the stack effect. For low values of the wind speed, displacement ventilation is maintained and a stratified interior is established. For a drainage flow, Hunt & Linden (1996), following a similar analysis to that presented by Linden et al (1990), show that the time evolution of the interface height h, as a fraction of the total height H over which the buoyancy force acts, may be written in the form

$$\frac{h}{H} = \left(\sqrt{1 + Fr_0^2} - \frac{t}{t_e}\right)^2 - Fr_0^2, \tag{27}$$

where $Fr_0 = \sqrt{\Delta/\rho g_0' H}$ is the "initial" Froude number based on the initial density difference g_0' and the wind pressure drop Δ between the windward and leeward openings. The time t_e taken for the enclosure to empty under the influence of buoyancy forces alone is given by (14).

The total time T taken for the enclosure to empty with the wind assisting the buoyancy, relative to the time taken to empty under buoyancy alone, is then

$$\frac{\mathrm{T}}{t_e} = \sqrt{1 + Fr_0^2} - Fr_0^2, \tag{28}$$

and thus the draining time decreases as Fr_0 increases. For small values of the Froude number, (28) shows that the emptying time is the buoyancy emptying time minus the emptying time associated with the flushing of the space in a simply linear fashion. At larger values of the Froude number, the displacement flow is approaching the purely wind-driven limit, as only small changes in the total emptying time result from variations in g'. Here the density difference acts merely to keep the fluid stratified and maintain the displacement mode, and the wind provides the dominant expelling force. The Froude number at time t may be expressed as

$$Fr(t) = Fr_0 \left(\frac{H}{h(t)} \right)^{\frac{1}{2}}, \tag{29}$$

and hence, for a constant wind velocity and density difference, the Froude number increases as the enclosure empties so that wind effects become increasingly dominant as the thickness h of the ambient layer increases.

It is observed that the two-layer stratification is maintained for a wide range of wind speeds. However, if the wind blows hard so that the wind-induced velocity is large compared with the buoyancy-induced velocity, then the displacement flow breaks down and the resulting flow is less efficient than the no-wind flow at flushing the buoyant fluid from the space. A minimum emptying time for flushing the space is found to occur at a critical initial Froude number Fr_{crit}, which is found to depend solely upon the geometry of the enclosure and is given by

$$Fr_{crit} = \sqrt{\left(\frac{a_W^{3/4}}{A^* H^{1/2} \delta} \left(H - \frac{h_L}{2} \right) \right)^2 - 1}, \tag{30}$$

where a_W denotes the area of the windward opening, h_L the height of the leeward opening, and δ is an empirical constant ($\approx$1.85) obtained from experiments.

5.1.2 SINGLE SOURCE OF BUOYANCY For the case of a single source of buoyancy within the space, the effect of wind is to increase the volume flow rate through the space. Consequently, in order to transport fluid across the interface in the plume, it is necessary that the interface rise within the space to achieve the required volume flux. GR Hunt & PF Linden (submitted) show that the

position of the new interface is given by

$$\frac{A^*}{H^2} = \frac{C^{3/2}\xi^{5/3}}{\left(\frac{1-\xi-d_c/H}{\xi^{5/3}} + CFr^2\right)^{1/2}}, \tag{31}$$

where here the Froude number Fr, given by

$$Fr = \sqrt{\frac{\Delta/\rho}{(B/H)^{2/3}}}, \tag{32}$$

is a measure of the relative magnitudes of the wind and buoyancy produced velocities.

In contrast to purely stack-driven displacement flows, when a stack-driven flow is assisted by wind, the position of the interface depends not only on the dimensionless area of the openings but also on the strength of the source; see (31) and (32). However, the interface height is a weak function of the source strength B.

The effect of the wind on the stack-driven flow is threefold: the interface is raised, there is a reduction in the temperature step across the interface, and an increased airflow rate through the space. Therefore, if the wind flow can be harnessed to assist the stack-driven flow, "passive" cooling may be achieved—(increased Q, lower ΔT, and more building fabric exposed to ambient air to enhance cooling—see Hunt & Linden 1997a).

5.2 *Opposing Wind and Buoyancy Forces*

5.2.1 DRAINAGE FLOWS Hunt & Linden (1997b, and paper in preparation) have conducted experiments to examine the ventilation of an enclosure by the opposing forces of wind and buoyancy. When the buoyancy force initially exceeds the dynamic pressure force of the oncoming stream, i.e. for $Fr_0 < 1$, three distinct flow regimes are observed. Initially, an outflow of buoyant fluid through the high-level, windward opening (i.e. into the oncoming stream) occurs. This fluid is replaced by denser wind-driven fluid, which enters through the low-level, leeward opening, i.e. a displacement flow is set up. As buoyant fluid is displaced from the space, the buoyancy force exerted at the high-level, windward opening decreases until it matches the dynamic pressure force of the wind-driven flow.

At this stage, oscillatory flow is observed. There are periods of exchange flow and periods of inflow at the windward opening. Initially, the observed exchange flow is not balanced but is predominantly outflow. As buoyant fluid continues to empty, the amount of inflow increases until there is entirely inflow. Fluid enters the enclosure as a negatively buoyant plume, which partially mixes with the warm layer, thereby increasing its density and creating wave-like disturbances on the fluid interface. The mixing between the incoming fluid and the fluid

contained in the enclosure causes the interface to descend. Once the interface reaches the bottom of the enclosure, a mixing-type ventilation flow then ensues, with an inflow of cool ambient fluid through the windward opening and outflow through the leeward opening. At this stage there is no significant stratification in the enclosure and the average density decays at an exponential rate as given by

$$\frac{g'}{g'(t_{full})} = -\frac{4kFr(t_{full})^2 e^{-\lambda(t-t_{full})/\tau}}{(1-ke^{-\lambda(t-t_{full})/\tau})^2}, \tag{33}$$

where the parameter k is given by

$$k = \frac{\sqrt{Fr(t_{full})^2 - 1} - Fr(t_{full})}{\sqrt{Fr(t_{full})^2 - 1} + Fr(t_{full})}$$

and

$$Fr(t_{full}) = \frac{1}{Fr_0}\sqrt{Fr_0^2 + h_W/H}$$

denotes the Froude number when the interface reaches the floor, at which time the buoyancy is $g'(t_{full})$ and h_W denotes the height of the windward opening.

The time scale τ is defined as $\tau = \frac{V}{A^*\sqrt{\Delta/\rho}}$, so that bigger openings, smaller enclosure volume, and stronger wind imply faster decay in temperature. Note that if the strength of the wind now decreases, so that the buoyancy force exerted at the windward opening exceeds the dynamic pressure force of the wind, then the entire ventilation flow sequence described above would be repeated.

For $Fr_0 > 1$, i.e. when initially the dynamic pressure force of the wind exceeds the buoyancy force exerted at the high-level windward opening, dense fluid enters the space through the windward vent and flows out the leeward vent. A mixing-type ventilation flow is established in this case, and the average density decays as in (33) with $Fr(t_{full})$ replaced by Fr_0.

5.2.2 SINGLE SOURCE OF BUOYANCY An interesting flow occurs in displacement ventilation with a single source when an opposing wind field is added. Consider the case where the interface is at a steady position in the absence of wind. When the wind begins to blow, the flow through the space is reduced and, as a consequence, the interface lowers so that the plume volume flux matches the reduced flowrate through the space. Above a critical wind speed, the flow is completely reversed, the interface comes down to the floor of the space, and a mixing flow develops. In the ensuing steady state, outflow is through the leeward openings and inflow through the windward openings. During the mixing flow, dense ambient fluid is driven into the space through the high-level windward openings and buoyant fluid is flushed through the low-level leeward openings.

Once this situation has occurred there remain two possibilities. The first is that at the imposed flow rate and temperature difference the heat flux from the space exceeds that input by the heat source. In this case the temperature in the space decreases with time, the flow rate increases until the heat flux equals that of the source, and a steady state is reached with the temperature given by (11). (Note that since the stack-driven flow is proportional to $\Delta T^{\frac{1}{2}}$ the heat flux will decrease even though the flow rate increases).

The second case is when the wind-driven flow is relatively weak and the heat flux from the space is less than that from the heat source. Then the temperature within the space will increase and the flow rate will decrease. As the temperature rises, the buoyancy-driven flow will increase and eventually the weak wind-driven flow will cease and then the flow through the space will reverse again to its original direction. A new displacement mode is established with the interface now in a new position given by

$$\frac{A^*}{H^2} = \frac{C^{3/2}\xi^{5/3}}{\left(\frac{1-\xi-d_c/H}{\xi^{5/3}} - CFr^2\right)^{1/2}}. \tag{34}$$

The above discussion shows that the behavior in the case of an opposing wind can be quite complex. It is also the case (GR Hunt & PF Linden, in preparation) that the behavior depends on the timescale over which the wind field is imposed. If the opposing wind is introduced gradually, then displacement ventilation may be established over the whole of the period, while if it is imposed rapidly, the transition may be such that mixing ventilation is obtained and the final state is then different from the case of the gradually applied wind. This hysteresis behavior is inherent in the nonlinear response of the pressure distribution to the wind field and leads to complex time-dependent effects still under investigation.

These studies have shown that the presence of stratification strongly influences the flow patterns within the space even when the wind-driven ventilation is the dominant force. It then remains to determine under what conditions the stratification within the interior is sustained in the presence of wind forcing.

5.2.3 THE TRANSITION BETWEEN DISPLACEMENT AND MIXING VENTILATION

At high wind speeds, it is possible that the wind-driven flow within the space may be strong enough to destroy a stable stratification and generate a mixed interior. The exact mechanism by which this may occur is complicated and depends on the form and strength of the stratification and the flow distribution within the space. To get a global estimate of the required flow rates, we use the concept of mixing efficiency (Linden 1979), which has been developed in other, more geophysical, contexts.

Broadly speaking it is known that turbulence is an inefficient mixer in the sense that at most only a small fraction (around 20%, but often much smaller;

see, for example, Holford & Linden 1998) of the turbulent kinetic energy is used to mix the stratification, thereby increasing the potential energy. The majority of the turbulence kinetic energy is dissipated by viscosity.

Consider a space with a two-layer stratification with a reduced gravity across the interface of g'. Suppose, for simplicity, the interface is at mid-depth in the space. If the height of the space is H and the floor area (assumed constant) is S, then the increase in potential energy when this stratification is completely mixed is

$$\Delta PE = \frac{1}{8}\rho g' H^2 S. \tag{35}$$

If the flow through the space is at a rate of Q, through openings with area A, the kinetic energy within the volume is

$$\Delta KE = \frac{1}{2}\rho \frac{SHQ^2}{A^2}. \tag{36}$$

The mixing efficiency, defined as $M = \frac{\Delta PE}{\Delta KE}$, is

$$M = \frac{g' H A^2}{4Q^2}. \tag{37}$$

For a buoyancy-driven flow without wind, $Q \sim \frac{1}{2}A(g'H)^{\frac{1}{2}}$ and so $M \sim 1$. To achieve a mixing efficiency of order 0.2 (a generous estimate) means that the wind-induced ventilation must increase this flow rate by a factor of two or three. Such large inflows of wind-driven ventilation are usually not permitted because of discomfort to the occupants, and this analysis suggests that the interior stratification plays a dominant role in determining the flow patterns within the space even on windy days. Hence, considerations of the combined effects of wind and buoyancy are crucial to the performance of naturally ventilated buildings.

6. COMPUTATIONAL FLUID DYNAMICS (CFD)

The use of CFD in calculating ventilation flows is becoming an increasingly common practice in the design of ventilation systems for new buildings (see reviews by Liddament 1991 and Jones & Whittle 1992). This work began in the 1970s (Nielsen 1974, 1980; Gosman et al 1980) with modeling of flow driven by inlet jets in simple geometries. Comparisons were made with laser-doppler anemometer measurements in a small-scale room. Other studies (e.g. Nielsen et al 1979, Nansteel & Grief 1984, Awbi 1989, McGuirk & Whittle 1991) extended this work, including some effects of buoyancy and further comparisons with experiments. Complex spaces have been considered by Yau & Whittle

(1991) with an application to an airport terminal and Harral & Boon (1993) to a pig house; and the use of body-fitted coordinates has been developed by Murakami & Kato (1989). In all these cases, the flows into and out of the enclosure are fixed, so they represent wind-driven natural ventilation, with a constant wind speed. The effect of buoyancy on the flow rate is ignored, with the exception of the work of Schaelin et al (1990), who modeled one-sided ventilation with a steady wind and a heat source. The results were found to be sensitive to the external pressure conditions, as was also found by Cook & Lomas (1998) (see below). Several commercial codes are available that solve the three-dimensional Navier-Stokes equations in some approximate form–laminar or Reynolds-averaged.

A major advantage of CFD is that it has the potential to provide detailed flow patterns and temperature distributions throughout the space, and the calculations can, in principle, include all the likely physical processes such as heat transfer from surfaces and transient behavior. CFD can also, in principle, deal with the complex geometry of a space and the arrangement and distribution of heat sources.

In practice, however, it is necessary to make simplifications to the geometries considered, and the finite grid means that processes such as heat transfer from surfaces have to be treated in an approximate way. Computational demands are heavy, and financial constraints impose limitations on the resolution of the calculations.

All commercial CFD codes use some form of turbulence modeling. At the lowest order, simple eddy viscosities are used to calculate turbulent momentum transports and eddy diffusivities for the transport of scalars. The next level of sophistication is to use a two-equation model such as the k-ε turbulence model in which transport equations for the turbulent kinetic energy k and its rate of dissipation ε are used, and there is a relationship between k and ε at each grid node. This method requires a set of modeling constants, which have been established by experiment, and in general, this treatment is relatively robust. This is the standard approach, and in situations where the geometry is fairly well defined and controls many aspects of the flow, it seems to work quite well. A more sophisticated version of the k-ε model is the RNG version in which the constants are derived using mathematical theory including the addition of a term in the dissipation equation related to the total rate of strain and the turbulent viscosity. This addition comes from Re-Normalization Group theory and it appears to be able to model some aspects of stratification.

Alternative closure forms are concerned with the transport of the Reynolds stresses and are termed either algebraic stress models or Reynolds stress transport models. In both of these models, equations for the Reynolds stresses are derived from Reynolds averaging and various assumptions are used to relate

these to the Reynolds stresses themselves. These flows have the ability to represent non-isotropic turbulence but are computationally very intensive and have additional complexities for the boundary conditions. These models have not been tested against data to the extent that the k-ε models have been.

Further approaches are to use large eddy simulations in which the smaller scales are averaged using a filter related to the size of the grid used to simulate the flow field.

It is not my intention here to discuss the merits, or otherwise, of particular codes. Nor do I intend to compare CFD calculations with other, apparently simpler models of ventilation. All models involve some degree of approximation, whether it is in assuming that heat sources give rise to pure plumes, or whether the grid-resolution in a CFD calculation is sufficient.

What is of interest, given that CFD codes are bound to continue to be refined and improved, is the fluid dynamical and ventilation issues that need to be addressed. Cook (1998) and Cook & Lomas (1998) have carried out a comprehensive study of one code, CFX, and compared the results of calculations with the experiments of a single plume in a space under displacement ventilation. Both two-dimensional and three-dimensional simulations have been conducted of the small-scale experiments using parameters appropriate to salt in water and for larger-scale experiments using heat in air. Careful comparisons have been made with the experimental results of Linden et al (1990). These show the qualitative behavior found in that case, that the interface height is independent of the heat flux at the source, is reproduced in the numerical calculations both in 2D and 3D. The main differences between the 2D and 3D simulations were associated with small differences in the plume entrainment rate, with lower values in the 3D case possibly resulting from the solid boundaries at the end of the plume. This resulted in increased interface heights and higher values of g'.

Two different turbulence models were used: a standard k-ε and the RNG k-ε, which takes account of buoyancy production and dissipation of turbulence. The results differed slightly between the two models: There seems to be evidence that the RNG k-ε performs better, but the differences were small compared with differences produced by changes in the distribution of grid resolution and specification of the far-field boundary conditions external to the space. The latter was carefully chosen to permit convergence of the solution to a steady state.

It is possible to achieve qualitative and quantitative agreement between the calculations and the experiments. Flows with strong buoyancy effects, both convection and stable stratification, place large demands on CFD codes and are generally outside the class of flows used in validation tests. The time taken to reproduce what are quite simple experiments was several man-months of effort—considerably greater than the experiments themselves.

Even when CFD calculations provide accurate answers to ventilation flows, the question still remains of how these will be used in building design. The designer requires an intuition of the likely effects of changes in the design or the operation of a building. Even specific answers from each design option will not provide that, and for the present generation of CFD codes, this is a very expensive option. One possibility is to consider coarse-resolution CFD calculations as a substitute for zonal modeling.

7. VENTILATION OF FIRES

Fires generate hot gases and other combustion products, usually at quite high temperatures. A relatively small fire will produce temperatures above 1000°C, and the density of this hot gas is about one quarter that of air. Such strongly buoyant flows are capable of carrying smoke particles and are non-Boussinesq.

From the point of view of escape of personnel, the transient response to the fire is the critical issue. This often consists of a rising plume that, when it hits the ceiling, spreads across it as a gravity current. When it reaches the other side of the space, a filling-box flow is generated, with the hot layer descending as more combustion products reach the ceiling. In these cases usually the biggest danger, particularly in tall spaces, is produced by obscuration caused by smoke particles that fall out of the hot layer. Little is known about this process, although analogous experiments have been carried out in other contexts such as sediment-laden river water entering the sea (T Maxworthy, in preparation). The heavy particles descend at a rate much greater than their Stokes' settling velocity because they generate local, negatively buoyant convection within the layer, somewhat equivalent to biological convective systems.

The long-term behavior, more relevant to the resistance of the fabric to the fire, depends on the ventilation system. In displacement mode, the behavior is qualitatively similar to the Boussinesq case in that a two-layer stratification forms.

Non-Boussinesq buoyant plumes entrain less rapidly than their Boussinesq counterparts. This has been known empirically for many years (Ricou & Spalding 1961), but only recently has the dependence of the entrainment rate u_e on the density ratio

$$u_e \propto \left(\frac{\rho}{\rho_a}\right)^{\frac{1}{2}} w, \tag{38}$$

where ρ is the plume density, ρ_a the ambient density, and w the mean vertical plume velocity, been shown to be consistent with similarity theory (Rooney & Linden 1996). This dependence of the entrainment on the density in the plume means that the volume flux in the plume depends on the source strength, and

hence, so does the interface height. As shown by Rooney & Linden (1997), the expression for the dimensionless interface height ξ is as given in (15) but with the effective area A^* modified to

$$A^* = \frac{\Theta^{\frac{1}{2}} c_d a_t a_b}{\left(\frac{1}{2}\left(\frac{c_d^2}{c} a_t^2 + a_b^2\right)\right)^{\frac{1}{2}}}, \tag{39}$$

where $\Theta = \frac{\rho}{\rho_a}$. In the Boussinesq limit $\Theta \to 1$ and the earlier results (16) are recovered. In the non-Boussinesq case, since the plume density depends on the heat flux from the fire, the interface height is no longer independent of the heat input. In practical terms these effects are relatively weak and the non-Boussinesq approximation is adequate except for extremely vigorous fires.

8. COMPLEX EFFECTS

The discussion so far has been restricted to simple cases concerning the ventilation of a single space and concentrated on steady-state ventilation régimes. As the discussion in Section 5 indicated, complicated time-dependent effects can occur and there are a range of other issues concerning multiply connected spaces, non-adiabatic walls, and heat source distributions that deserve further comment.

8.1 *Time-Dependent Flows*

Here we discuss the response of displacement ventilation to the sudden introduction of a heat source into a space initially at ambient temperature. Such a flow would be established, for example, when a large number of people enter an auditorium, and since the ventilation system for auditoria are usually designed on steady-state conditions, it is of interest to see whether this is appropriate during the transient warm-up phase of the space. For the case of a single heat source, the analysis is straightforward (Hunt & Linden, 1998). The hot air generated by the source accumulates at the ceiling—this phase is a filling box phase and involves gravity currents spreading along the ceiling before the flow begins to exit through an upper-level vent. The exact flow details here are dependent on the aspect ratio of the space (Baines & Turner 1969). Once an outflow begins, cool air is introduced at low level and a displacement ventilation pattern is established. Since the interface is near the top of the space initially, the flow in the plume at that height is not matched with the inflow. Consequently, more warm fluid is added to the upper layer and the interface descends. It is shown by both experiments and theoretical analysis that the descent continues below the ultimate steady-state level since, when the interface reaches the steady-state level, the upper layer is not uniform in temperature and is cooler than the final steady-state temperature. Consequently, the flow through the openings does

not match the plume volume flux and the interface continues to descend and the upper layer continues to warm. A minimum in the interface level is achieved as the outflow through the openings increases, and eventually the interface reaches its equilibrium steady-state position. The amount of overshoot depends on the surface area S of the floor of the space, and the timescale τ_s for the establishment of the steady state is given by

$$\tau_s = \frac{S}{B^{\frac{1}{3}} H^{\frac{2}{3}}}. \tag{40}$$

Thus the steady-state timescale increases with the area of the space but decreases with increasing height and buoyancy flux from the source. The dependence on the cross-sectional area implies that in spaces in which this area is not constant, such as in a lecture room where there is tiered seating so that the cross-section area increases with height, the interior geometry may affect the timescale and the amount of overshoot before the establishment of the steady state. This will only be the case if the upper warm layer extends down into the region of non-constant cross-section. Consequently, calculations that ignore blockages to the cross-sectional area, such as those produced by furniture, machinery, occupants, etc, in the lower part of the space, will still give accurate estimates of the time-dependent behavior and the depth of the final steady-state provided the interface never enters this region. Since the latter condition is the design criterion, this property leads to simple design rules.

Calculations for a lecture theater occupied by some 500 people suggest that the timescale for the establishment of the steady state is about one hour (Hunt & Linden 1998). This implies that the design criteria should be developed to account for the additional lowering of the interface during the transient behavior rather than just simply on the final steady-state interface value.

Similar considerations can be made to consider the effects of time-varying heat sources and also the effects of time-varying wind strengths.

8.2 *Multiply-Connected Spaces*

The possibility of multiply-connected spaces leads to a new class of problems. Since each space has its own timescale associated with the volume and the flow rate through the space and the detailed flow patterns depend on the connections between the spaces, a new class of problems presents itself that has received virtually no attention. One exception is the work of Gladstone et al (1998), who considered a combination of displacement ventilation with the incoming air being able to exchange through an opening into a second chamber. They developed a model that combined the ideas of displacement ventilation from Linden et al (1990) with a hydraulic exchange (Dalziel & Lane-Serff 1991) and showed how the interface varied as a function of time. This work was

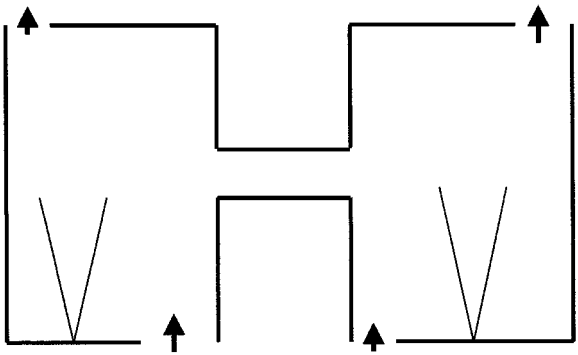

Figure 8 A schematic of two connected spaces illustrating the possible range of conditions that could be investigated.

supported by small-scale experiments using salt water and raises a number of interesting questions concerning the interactions between the two spaces. It is clear that a classification of these problems is desirable. None such has yet been attempted.

Figure 8 shows an example of a canonical problem in which the various openings and geometry allow a wide range of flows to be established. This figure shows two chambers with a single connection and with openings in the top and bottom of each chamber. The simplest case to consider is two equal heat sources, one in each space, and with equal openings in each space. This case is clearly exactly the same as that shown in Figure 3 for the single space with no effective exchange between the two spaces. By varying the openings in one of the chambers relative to the other, different flow rates in the two chambers can be established and an exchange flow through the connection will be developed. The nature of the exchange flow will depend on the height of the interface relative to the height of the single opening between the two chambers. Other possible developments of this problem would be to have plumes of different strengths and to consider multiple openings between the two chambers. It would also be possible to imagine mixing ventilation in one chamber and displacement ventilation in the other. By building up intuition on this class of flows it is possible to develop significant insights into the ventilation of complex buildings.

8.3 *Non-Adiabatic Walls*

The other feature apart from the air movement that determines the ventilation and comfort levels in the indoor space is the building fabric. The discussion so far has concentrated on walls that are totally insulating with no heat exchange

with the fabric surrounding the space. Increasingly, heavy materials are used as heat storage usually in harness with night cooling as a means of providing additional cooling during high daytime temperatures. A massive structure such as an exposed concrete roof will be cooled by ventilating the building at night, and the following day this storage of negative heat will be used to extract heat from the air within the space providing the required cooling. There appears to be very little work on the effect of heat transfer from walls on the ventilation flow. Experiments have been conducted by Sandberg & Lindstrom (1990), who measured temperature profiles in displacement ventilation with adiabatic walls and with walls that are heated and cooled. They observed changes in the temperature profile but more importantly changes in the position of the interface in displacement ventilation according to the cooling or heating of the walls. Their observations show a small rise in interface height with wall cooling. This is a result of downflow at the walls generated by the cooling requiring an additional upflow in the plume to match the volume flow through the space. (This is forced ventilation at a fixed flow rate.) This increased flow rate is achieved by having the interface higher up the space. Some experiments on single-sided ventilation using a heated room have been carried out by van der Maas et al (1990). They developed a model based on gravity current flow plus heat extraction from the wall and showed that it is possible to develop wall space that is covered by cool fluid and is therefore exchanging heat with the boundary.

Nevertheless, there are no systematic rules developed for incorporating the effects of non-adiabatic boundaries. This problem is of significant practical importance. One of the difficulties is that the laboratory experimentation on small scales makes it difficult to match the boundary-layer structure, particularly on vertical walls. In a full-scale building, the boundary layer is likely to be laminar for the lower part of the flow next to a heated wall and then become turbulent at some height above the floor, usually a meter or so. Since the heat transfer varies dramatically with the transition from laminar to turbulent flow, this process is difficult to model exactly in the laboratory. Nevertheless, this is clearly an important area deserving further attention.

8.4 *Plume Interactions—Realistic Sources*

The discussion concerning heat sources has been restricted to very idealized cases of pure plumes generated at the bottom of the space. In practice, heat sources are far more complex both in their geometrical arrangement as they may be distributed, associated with, for example, sun patches shining on the floor or on walls and also because they may occur at different elevations within the space. While it is reasonable to assume that these divergences from the idealized plume may be taken into account by using virtual origins and making

the appropriate correction for plumes raised above the floor, there are some significant unresolved questions concerning the representation of heat sources in practice. The controlling feature of the ventilation in displacement mode is the volume flux carried by the plume. This is a result of entrainment. Consequently, arrangements in which the entrainment into a plume is significantly altered will make substantial differences to the interface height and need to be considered. One obvious example is a plume near a boundary, and particularly in a corner, where the entrainment is cut off by the walls and so reduced from that of an unobstructed axisymmetric plume.

Another possibility receiving attention (Kaye 1998) is the question of plume interaction. In most buildings there are multiple heat sources, and while these have been discussed in Section 3.1, it has been assumed that the plumes rise independently of one another. Since plumes entrain the ambient fluid between them, they are naturally drawn together and will merge if sufficiently close together as they rise. Kaye (1998) has shown that the merging process is a strong function of the separation of the heat sources and that, for plumes of equal strength, merging takes place about three to four source separations above the source. For unequal plumes, merging takes place sooner, as the weaker plume is drawn into the stronger plume. Once the two plumes have merged, the total buoyancy flux is conserved, but the volume flux in the single plume is less than would be carried in the two separate plumes. Consequently the interface will be higher for a merged plume than it would be for the two separate plumes. Other applications of this work concern the interaction of opposing plumes such as those from a chilled ceiling interacting with heat rising from the floor. Again, it is found (Kaye 1998) that the collision is a strong function of the horizontal separation of the two sources. It is possible to account for the additional mixing between the two plumes using an entrainment model.

9. CONCLUDING REMARKS

In this review I have attempted to summarize the problems and research associated with the natural ventilation of buildings. The motivation behind this work has been to provide designers, architects, and mechanical ventilation engineers with guidance to develop efficient natural ventilation systems. This guidance can take two forms, both of which, I contend, are important to the use of natural ventilation as a viable form of ventilating buildings. The first concerns formulae and rules for estimating the openings, their placement, and the consequent flow rates necessary for the design of an efficient building. Most designers will have an idea of the required air changes per hour that they wish to achieve in any particular space, and the research is aimed at showing how these air changes may be achieved by appropriate use of openings. The second part of

this guidance, which I believe to be equally important, is to develop an intuition for the way air moves around a building and how this is affected by changes in the design and in the external conditions. This is a more difficult aspect of the guidance to transmit, and for this purpose laboratory experiments in which flow patterns are illustrated are an extremely useful tool. They show designers, often in an idealized form, the types of flows that will be generated within a space when there are stack-driven and wind-driven effects. The ability to observe these flows is a major step in developing an understanding about how air moves around a building, which is the essential ingredient in designing the ventilation system. Laboratory experiments have also been very instructive in defining for fluid dynamicists the kinds of flows that need to be analyzed. The observation of ventilation flows in the laboratory makes it possible to develop models that give the required design rules.

In addition, this study of ventilated spaces has presented new fluid flows of intrinsic interest. They couple together almost every aspect of stratified flows. Canonically there are three forms of stratification which, if we consider the simple case of two layers separated by an interface, are: the horizontal interface with the denser fluid below (stable stratification), the horizontal interface with denser fluid above (unstable stratification), and a vertical interface separating regions of different density (the gravity current). All these types of stratification and their consequent dynamical behaviors operate in buildings: buoyant convection leading to rapid vertical mixing and rapid transport; stable stratification, which inhibits vertical mixing and reduces vertical transport; and gravity current behavior, which leads to rapid horizontal exchanges within the space. Of these three, stable stratification is the persistent feature, the other two leading to rapid motion and redistribution of the density field toward the stable case. Buoyant fluid accumulates at the ceiling, producing stable stratification via the "filling box" process, while the gravity current makes dense fluid run underneath light fluid, again producing stable stratification. We have seen that stable stratification is an intrinsic ingredient in the displacement ventilation flow. Only by breaking this up is it possible to develop mixing ventilation; special measures have to be taken for that to occur. So stratification plays a very strong role in the flow patterns established within a building, and even though wind effects appear to be dominant on the basis of simple pressure variations from the top to bottom of a building and the windward to leeward faces, it is nevertheless clear that internally, partly because the wind is diminished by closing down vents, the stratification determines the flow patterns in most cases.

ACKNOWLEDGMENTS

One of the excitements of this research is the possibility of working on real buildings and I am indebted to many people, particularly Nick Baker, Brian

Ford, and François Penz, for the opportunities to work with them and to learn about architectural concerns. I have also benefited enormously from interaction with colleagues and research students who have worked with me on ventilation problems, particularly Paul Cooper, Gavin Davies, Joanne Holford, Gary Hunt, Gregory Lane-Serff, David Smeed, and John Simpson. Finally, I wish to thank Susan Messenger for her help with the preparation of this article.

Literature Cited

Awbi HB. 1989. Application of computational fluid dynamics in room ventilation. *Build. Environ.* 24:73–84

Baker N, Linden PF. 1991. Physical modelling of airflows—a new design tool. *Atrium Build. Archit. Eng.* 13–22, Ed. F. Mills. CICC Publications, Welwyn, England

Britter RE, Hunt JCR, Mumford JC. 1979. The distortion of turbulence by a circular cylinder. *J. Fluid Mech.* 92:269–301

Baines WD, Turner JS. 1969. Turbulent buoyant convection from a source in a confined region. *J. Fluid Mech.* 37:51–80

Brown WG, Solvason KR. 1962a. Natural convection heat transfer through rectangular openings in partitions-I. *Int. J. Heat Mass Transf.* 5:859–68

Brown WG, Solvason KR. 1962b. Natural convection heat transfer through rectangular openings in partitions-II. *Int. J. Heat Mass Transf.* 5:869–78

Brown WG, Wilson AG, Solvason KR. 1963. Heat and moisture flow through openings by convection. *J. Am. Soc. Heat. Vent. Air Cond. Eng.* 5:49–54

Caulfield CP. 1991. Stratification and buoyancy in geophysical flows. PhD thesis. Cambridge Univ., UK

Cook MJ. 1998. An evaluation of computational fluid dynamics for modelling buoyancy-driven displacement ventilation. PhD thesis. de Montfort Univ., Leicester, England

Cook MJ, Lomas K. 1998. Buoyancy-driven displacement ventilation flows: evaluation of two eddy viscosity turbulence models for prediction. *Proc. CIBSE A: Build. Serv. Eng. Res. Technol.* 19:15–21

Cook NJ, Atkinson PA, Watts PA. 1974. Investigating localised urban wind conditions in full-scale using a mobile anemometer mast. *J. Fluid Mech.* 79:18–25

Cooper P, Mak N. 1991. Thermal stratification and ventilation in atria. *Proc. ANZSES (Australian and New Zealand Solar Energy Soc.) Conf., Adelaide, Australia,* pp. 385–91

Cooper P, Linden PF. 1995. Natural ventilation of an enclosure containing one positive and one negative source of buoyancy. *Proc. 12th Australas. Fluid Mech. Conf.*, Sydney, Aust. 645–48

Cooper P, Linden PF. 1996. Natural ventilation of an enclosure containing two buoyancy sources. *J. Fluid Mech.* 311:153–76

Dalziel SB, Lane-Serff GF. 1991. The hydraulics of doorway exchange flows. *Build. Environ.* 26:2:121–35

Dascalaki E, Santamouris M. 1996. Natural ventilation. In *Passive Cooling of Buildings*, ed. M Santamouris, D Asimakopoulis, pp. 220–306. London: James & James

Davies GMJ. 1993. Buoyancy driven flow through openings. PhD thesis. Cambridge Univ., UK

Davies GMJ, Linden PF. 1992. The effects of headwind on buoyancy-driven flow through a doorway. *Proc.* ROOMVENT'92, *3rd Int. Conf. Air Distrib. in Rooms, Aalborg, Denmark*, pp. 419–33

Epstein M. 1988. Buoyancy-driven exchange flow through openings in horizontal partitions. *Intl. Conf. Cloud Vapor Modelling, Nov. 1987, Cambridge, MA*

Evans RA, Lee BE. 1981. The problems of anemometer exposure in urban areas—a wind tunnel study. *Met. Mag.* 110:188–99

Gladstone C, Woods A, Philips J, Caulfield C. 1998. Experimental study of mixing in a closed room by doorway exchange flow. *Proc.* ROOMVENT'98, *Stockholm, Sweden*

Gorton RL, Sassi MM. 1982. Determination of temperature profiles in a thermally stratified air-conditioned system: Part 2. Program description and comparison of computed and measured results. *Trans. ASHRAE,* 88 (2), paper 2701

Gosman AD, Nielsen PV, Restivo A, Whitelaw JH. 1980. The flow properties of rooms with small openings. *J. Fluids Eng.* 102:316–23

Hacker J, Linden PF, Dalziel SB. 1996. Mixing in lock-release gravity currents. *Dyn. Atmos. Oceans* 24:183–95

Harral BB, Boon CR. 1993. Modelling the air flow and environment in a pig house. *AFRC Silsoe Res. Inst.*

Holford JM, Linden PF. 1998. The development of layers in a stratified fluid. *Proc. 5th IMA Conf. Stratified Flows*. Dundee, UK. In press

Hunt GR, Linden PF. 1996. The natural ventilation of an enclosure by the combined effects of buoyancy and wind. *Proc.* ROOMVENT'96, *5th Int. Conf. on Air Distrib. in Rooms.* 3: 239–46. Yokohama, Japan

Hunt GR, Linden PF. 1997a. Passive cooling by natural ventilation: salt bath modelling of combined wind and buoyancy forces. *Proc. AIVC*, Athens, Greece

Hunt GR, Linden PF. 1997b. Laboratory modelling of natural ventilation flows driven by the combined forces of buoyancy and wind. *Proc. CIBSE Nat. Conf.*, London

Hunt GR, Linden PF. 1998. Time-dependent displacement ventilation caused by variations in internal heat gains: application to a lecture theatre. *Proc.* ROOMVENT'98, *6th Int. Conf. on Air Distrib. in Rooms*, 2:203–10. *Stockholm, Sweden*

Hussain M, Lee BE. 1980. A wind tunnel study of the mean pressure forces acting on large groups of low rise buildings. *J. Wind Engng. Indust. Aerodyn.* 6:207–25

Jacobsen J. 1988. Thermal climate and air exchange rate in a glass covered atrium without mechanical ventilation related to simulations. *13th Natl. Solar Conf. MIT, Cambridge, MA*, 4:61–71

Jones PJ, Whittle GE. 1992. Computational fluid dynamics for building airflow prediction—current status and capabilities. *Build. Environ.* 27:321–38

Kaye N. 1998. Interaction of turbulent plumes. PhD thesis. Cambridge Univ., UK

Keil DE. 1991. Buoyancy driven counterflow and interfacial mixing. PhD thesis, Cambridge Univ., UK

Lane-Serff GF, Linden PF, Simpson JE. 1987. Transient flow through doorways produced by temperature differences. *Proc.* ROOMVENT'87, *Stockholm, Sweden*

Lane-Serff GF. 1989. Heat flow and air movement in buildings. PhD thesis. Cambridge Univ., UK

Liddament MW. 1991. A review of building air flow simulation. *Tech. Note AIVC 33*

Linden PF. 1979. Mixing in stratified fluids. *Geophys. Astrophys. Fluid Dyn.* 13:3–23

Linden PF, Cooper P. 1996. Multiple sources of buoyancy in a naturally ventilated enclosure. *J. Fluid Mech.* 311:177–92

Linden PF, Jagger SF, Redondo JM, Britter RE, Moodie K. 1992. The effect of a waterspray barrier on a tunnel fire. *Proc. I. Mech. E.* 1992:7:59–64

Linden PF, Lane-Serff GF, Smeed DA. 1990. Emptying filling spaces: the fluid mechanics of natural ventilation. *J. Fluid Mech.* 212:300–35

Linden PF, Simpson JE. 1985. Buoyancy driven flows through an open door. *Air Infiltration Rev.* 6:4–5

Linden PF, Simpson JE. 1987. Development of density discontinuities in a turbulent fluid. In *Stably Stratified Flows and Dense Gas Dispersion*, ed. J Puttock, pp. 97–115. Oxford, UK: Oxford Univ. Press

McGuirk JJ, Whittle GE. 1991. Calculation of buoyant air movement in buildings—proposal for a numerical benchmark test. *I. Mech. E. Conf. "Computational Fluid Dynamics—Tool or Toy,"* London

Maxworthy T. 1997. Convection into domains with open boundaries. *Annu. Rev. Fluid Mech.* 29:327–72

Morton BR, Taylor GI, Turner JS. 1956. Turbulent gravitational convection from maintained and instantaneous sources. *Proc. R. Soc. A* 234:1–23

Murakami S, Kato S. 1989. Numerical and experimental study on room airflow—3-D predictions using the k-ε turbulence model. *Build. Environ.* 24:85–97

Nansteel MW, Greef R. 1984. An investigation of natural convection in enclosures with two- and three-dimensional partitions. *Int. J. Heat Mass Transf.* 27:561–71

Nielsen PV. 1974. Flow in air-conditioned rooms. PhD thesis. Technical Univ. Denmark

Nielsen PV. 1980. The influence of ceiling-mounted obstacles on the airflow patterns in air-conditioned rooms at different heat loads. *Build. Services Eng. Res. Tech.* 1:

Nielsen PV, Restivo A, Whitelaw JH. 1979. Buoyancy affected flow in ventilated rooms. *Numer. Heat Transf.* 2:115–27

Owen PR. 1971. Buildings in the wind. *Q. J. R. Met. Soc.* 97:396–413

Ricou FP, Spalding DB. 1961. Measurements of entrainment by axisymmetrical turbulent jets. *J. Fluid Mech.* 8:21–32

Rooney GG, Linden PF. 1996. Similarity considerations for non-Boussinesq plumes in an unstratified environment. *J. Fluid Mech.* 318:237–50

Rooney GG, Linden PF. 1997. Strongly buoyant plume similarity and 'small-fire' ventilation. *Fire Saf. J.* 29:235–58

Sandberg H, Lindstrom S. 1987. A model

for ventilation by displacement, *Proc.* ROOMVENT'87, Stockholm, Sweden, June 10–12, 1987

Sandberg H, Lindstrom S. 1990. Stratified flow in ventilated rooms—a model study. *Proc.* ROOMVENT'90, Oslo, Norway, June 13–15, 1987

Savardekar K. 1990. Aspects of passive cooling. A study on natural ventilation. MPhil thesis. Cambridge Univ., UK

Schaelin A, van der Maas J, Moser A. 1990. Simulation of airflow through large openings in buildings. *ASHRAE trans.*

Shaw BH, Whyte W. 1974. Air movement through doorways—the influence of temperature and its control by forced airflow. *J. Inst. Heat. Vent. Eng.* 42:210–18

Thomas PH, Hinkley PL, Theobald CR, Simms DL. 1963. Investigations into the flow of hot gases in roof venting. *Fire Res. Tech. Paper 7*, HMSO

van der Maas J, Roulet C-A, Hertig J-A. 1990. Transient single-sided ventilation through large openings in buildings. *Proc.* ROOMVENT'90, Oslo, Norway

Wilson DJ, Keil DE. 1990. Gravity-driven counterflow through an open door in a sealed room. *Build. Environ.* 25:379–88

Yau RMH, Whittle GE. 1991. Air flow analysis for large spaces in an airport terminal building: computational fluid dynamics and reduced-scale physical model tests. *I. Mech. E. Conf. "Computational Fluid Dynamics—Tool or Toy,"* London

Annual Review of Fluid Mechanics
Volume 31, 1999

CONTENTS